

Strasbourg Astronomical Observatory Seminar

Compton Polarimetry of Gamma-Ray Transients: Insights from Gamma-Ray Bursts to Solar Flares

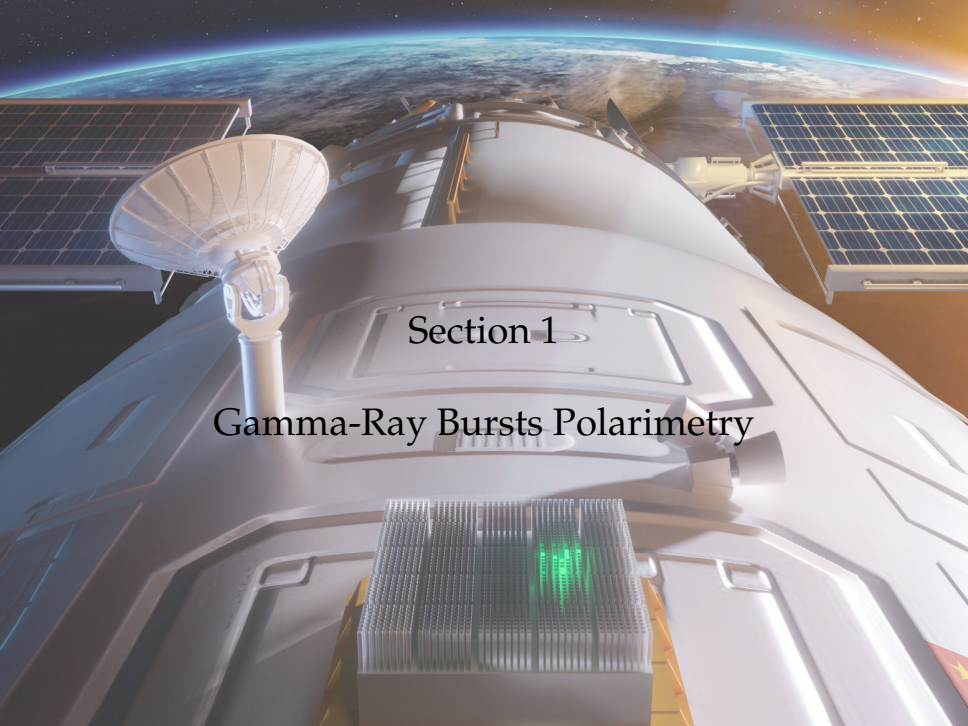
Nicolas De Angelis

INAF-IAPS, Rome, Italy (formerly at Uni Geneva)

March 28, 2025

Outline

- 1 Gamma-Ray Bursts Polarimetry
- 2 GRB Polarization Measurements from POLAR
- 3 Future of GRB Polarimetry with the POLAR-2 Mission
- 4 Solar Flare Polarimetry with the CUBesat Solar Polarimeter (CUSP)



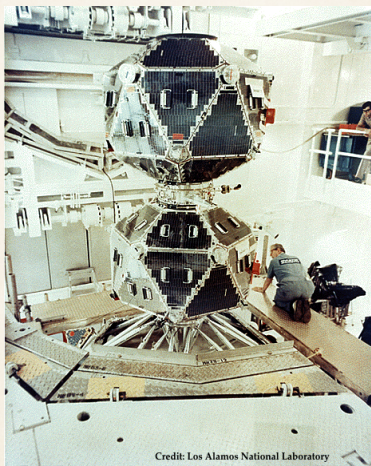
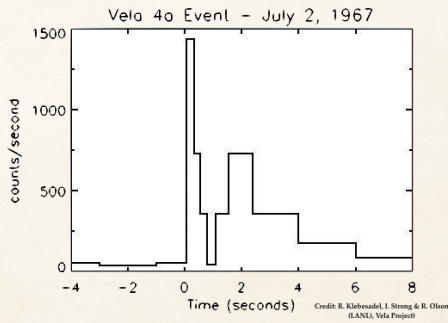
A detailed 3D rendering of a satellite in orbit around Earth. The satellite features a large white cylindrical body with various scientific instruments attached. A prominent feature is a white parabolic dish antenna mounted on a white cylindrical base. To the right, there are two large rectangular solar panels with a grid of blue cells. The background shows the blue and white atmosphere of Earth's horizon against the black void of space.

Section 1

Gamma-Ray Bursts Polarimetry

Discovery of GRBs

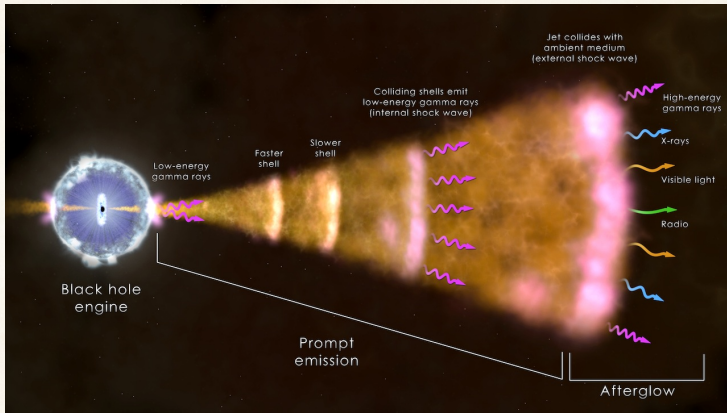
- Project Vela from USAF monitoring compliance to the Partial Test Ban Treaty of 1963
- First GRB detected on July 2nd, 1967 by Vela-4A, made public 7 years later
- Publication of 16 GRBs in 1973 by Klebesadel et al.



Credit: Los Alamos National Laboratory

The Gamma-Ray Bursts paradigm

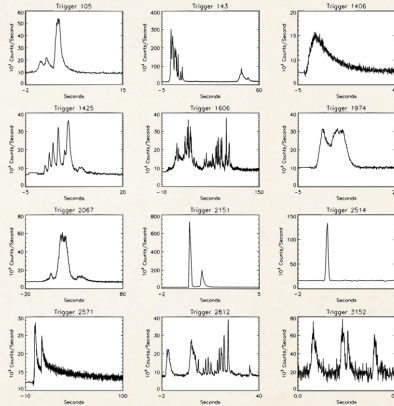
- Bright and short transient event in the γ band (**prompt emission**) followed by an **afterglow** spanning the entire EM spectrum



(Credit: NASA's Goddard Space Flight Center)

The Gamma-Ray Bursts paradigm

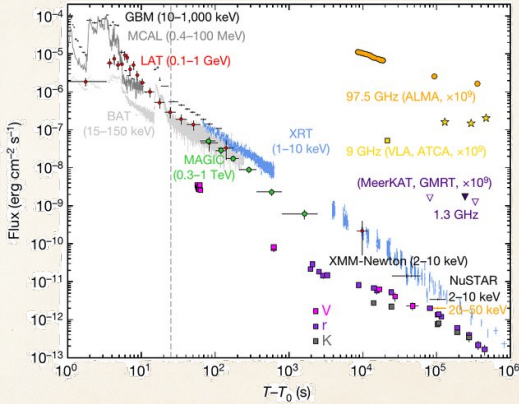
- Bright and short transient event in the γ band (**prompt emission**) followed by an **afterglow** spanning the entire EM spectrum



(Credit: J.T. Bonnell (NASA/GSFC))

The Gamma-Ray Bursts paradigm

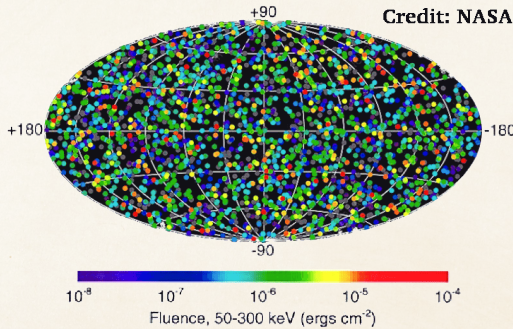
- Bright and short transient event in the γ band (**prompt emission**) followed by an **afterglow** spanning the entire EM spectrum



(Credit: MAGIC Collaboration, Nature 2019)

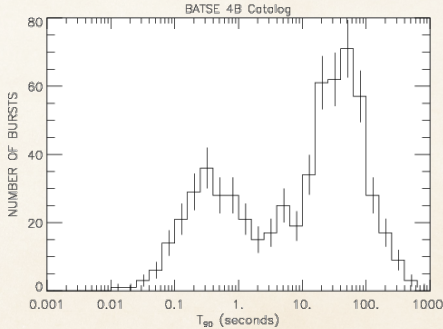
The Gamma-Ray Bursts paradigm

- Bright and short transient event in the γ band (**prompt emission**) followed by an **afterglow** spanning the entire EM spectrum
- GRBs are uniformly distributed in the sky, have very diverse spectral properties and fluence, and are of extragalactic origin



The Gamma-Ray Bursts paradigm

- ❶ Bright and short transient event in the γ band (**prompt emission**) followed by an **afterglow** spanning the entire EM spectrum
- ❷ GRBs are uniformly distributed in the sky, have very diverse spectral properties and fluence, and are of extragalactic origin
- ❸ Classified in two categories: short GRBs ($T_{90} < 2$ s) are originated by binary compact object merger, long ones ($T_{90} > 2$ s) are associated with supermassive star explosions

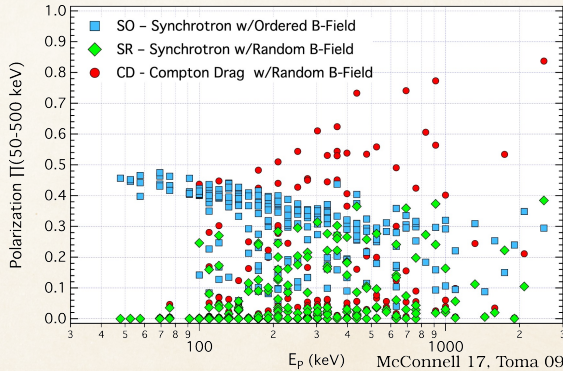


(Credit: BATSE 4B Catalog, Robert S. Mallozzi)

Why measuring GRB polarization ?

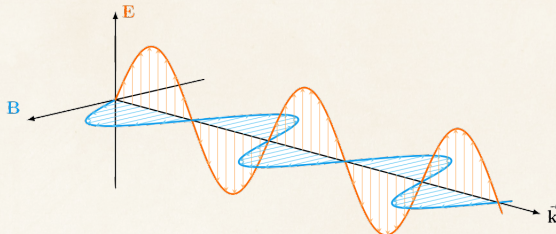
Spectral information alone does not allow to disentangle the existing emission models.
Measuring polarization is a very powerful tool to probe the physics of GRBs, as it can inform us about:

- ⌚ The emission mechanism at play in the source (synchrotron vs. photospheric)
- ⌚ The outflow dynamics: Kinetic Energy vs. Poynting Flux Dominated
- ⌚ The jet angular structure: top hat jet, with smooth edges, truly structured
- ⌚ The magnetic field configuration (random, ordered)



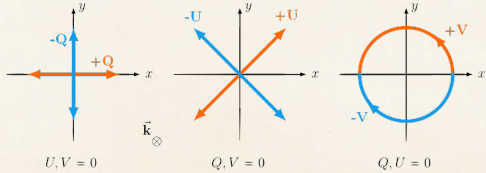
Polarization of Electro-Magnetic Waves

Stokes Parameterization



A photon consists of the propagation of orthogonal **E** and **B** fields. **E** is taken by convention as the polarization vector. Stokes parameterization of the polarization state:

$$\vec{S} = \begin{cases} S_0 \equiv I = \langle E_x^2 \rangle + \langle E_y^2 \rangle \\ S_1 \equiv Q = \langle E_x^2 \rangle - \langle E_y^2 \rangle \\ S_2 \equiv U = \langle E_{45^\circ}^2 \rangle - \langle E_{-45^\circ}^2 \rangle \\ S_3 \equiv V = \langle E_R^2 \rangle - \langle E_L^2 \rangle \end{cases}$$



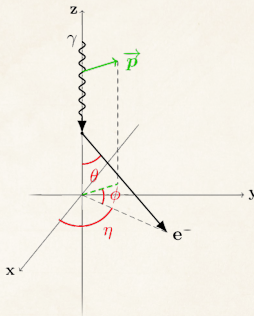
For a linearly polarized wave, polarization fraction and angle are defined by:

$$(PD[\%] \equiv PF \equiv) p = \frac{\sqrt{Q^2 + U^2}}{I}; \quad (PA \equiv) \psi = \frac{1}{2} \arctan \frac{U}{Q}$$

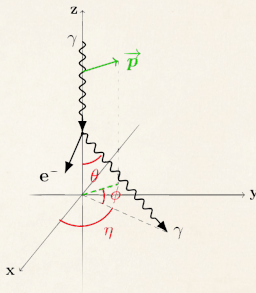
Photon interaction with matter

- Photon interaction with matter through three processes:

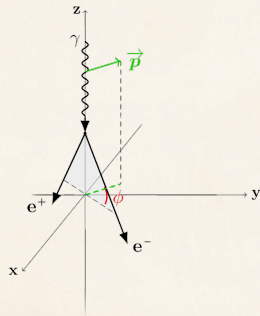
Photo-electric effect



Compton scattering



Pair production

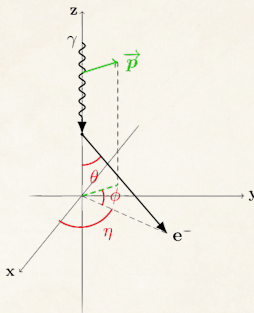


- Each process is dominant at different energies
- The azimuthal distribution of the secondary products is correlated with the polarization direction of the primary photon: $\frac{d\sigma}{d\Omega} \propto 1 + \mu \cos(2\phi)$

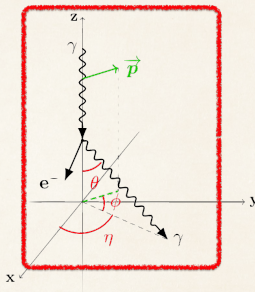
Photon interaction with matter

- Photon interacts with matter through three processes:

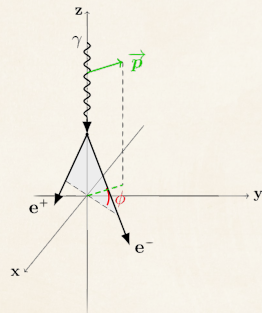
Photo-electric effect



Compton scattering



Pair production



- Each process is dominant at different energies
- The azimuthal distribution of the secondary products is correlated with the polarization direction of the primary photon: $\frac{d\sigma}{d\Omega} \propto 1 + \mu \cos(2\phi)$
- Compton scattering is the dominant process in the energy band where the GRB prompt emission and SF non-thermal emission peak

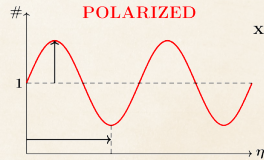
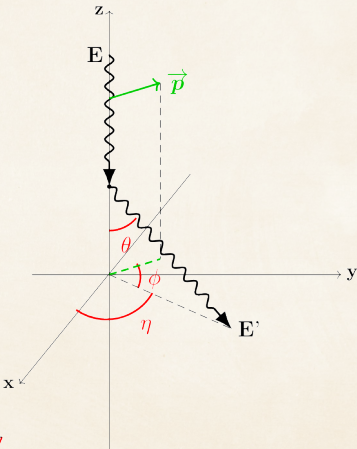
Compton Polarimetry

Compton scattering can be used to determine the polarization of a source:

- ⌚ Azimuthal scattering angle distribution provides information on PD and PA
- ⌚ Modulation curve parameterized by the Klein-Nishina cross-section:

$$\frac{d\sigma}{d\Omega} = \frac{r_e^2}{2} \left(\frac{E'}{E} \right)^2 \left[\frac{E'}{E} + \frac{E}{E'} - 2 \sin^2(\theta) \cos^2(\phi) \right]$$

- ⌚ Relative amplitude \leftrightarrow PD, phase \leftrightarrow PA



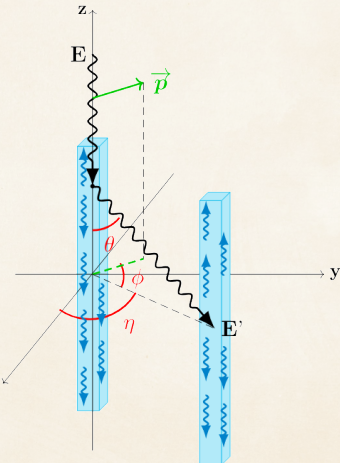
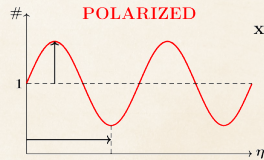
Compton Polarimetry

Compton scattering can be used to determine the polarization of a source:

- ⌚ Azimuthal scattering angle distribution provides information on PD and PA
- ⌚ Modulation curve parameterized by the Klein-Nishina cross-section:

$$\frac{d\sigma}{d\Omega} = \frac{r_e^2}{2} \left(\frac{E'}{E} \right)^2 \left[\frac{E'}{E} + \frac{E}{E'} - 2 \sin^2(\theta) \cos^2(\phi) \right]$$

- ⌚ Relative amplitude \leftrightarrow PD, phase \leftrightarrow PA
- ⌚ A segmented array of scintillators can be used to measure the scattering angle distribution (aka modulation curve)



Early GRB Polarization Measurements

GRB	Instrument	Energy (keV)	PD (%)
021206	RHESSI	150-2000	$80 \pm 20\%$
021206	RHESSI	150-2000	<100%
021206	RHESSI	150-2000	$41^{+57\%}_{-44\%}$
930131	CGRO/BATSE	20-1000	35-100%
960924	CGRO/BATSE	20-1000	50-100%
041219A	INTEGRAL/SPI	100-350	$98 \pm 33\%$
041219A	INTEGRAL/SPI	100-350	$96 \pm 40\%$
041219A	INTEGRAL/IBIS	200-800	$43 \pm 25\%$
061122	INTEGRAL/SPI	100-1000	< 60%
100826A	IKAROS/GAP	70-300	$27 \pm 11\%$
110301A	IKAROS/GAP	70-300	$70 \pm 22\%$
110721A	IKAROS/GAP	70-300	$80 \pm 22\%$
061122	INTEGRAL/IBIS	250-800	> 60%
140206A	INTEGRAL/IBIS	200-800	> 48%
151006A	Astrosat/CZTI	100-300	-
160530A	COSI	200-5000	< 46%

from McConnell 2016

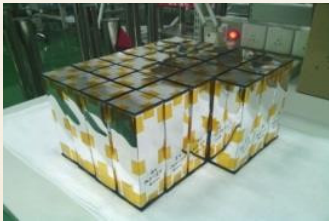
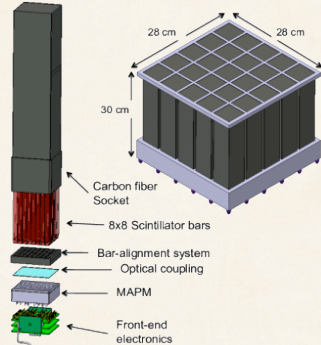


Section 2

GRB Polarization Measurements from POLAR

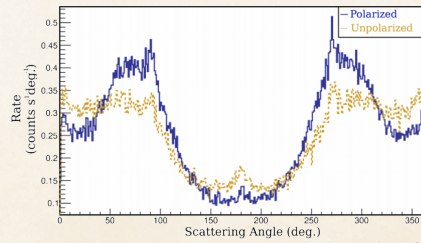
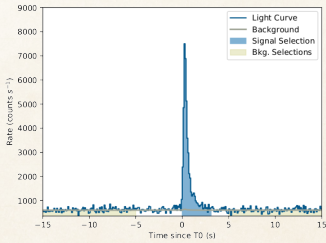
The POLAR Instrument

- ★ POLAR was a dedicated gamma polarimeter composed of a 40×40 scintillator array
- ★ Divided in 5×5 modules each made of 64 plastic scintillator bars ($176 \times 5.8 \times 5.8 \text{ mm}^3$, EJ-248M), each module being readout by Multi-Anode PMTs
- ★ Optimized for Compton scattering in the 50-500keV range thanks to its low-Z scintillators
- ★ 30kg instrument, half-sky FoV, $\sim 300\text{cm}^2$ effective area at 400 keV
- ★ Design described in Produit et al. 2018 (DOI: [10.1016/j.nima.2017.09.053](https://doi.org/10.1016/j.nima.2017.09.053))
- ★ Launched in Sept 2016 on the Tiangong-2 Chinese space lab for 6 months of operation



POLAR GRB Polarization Measurements

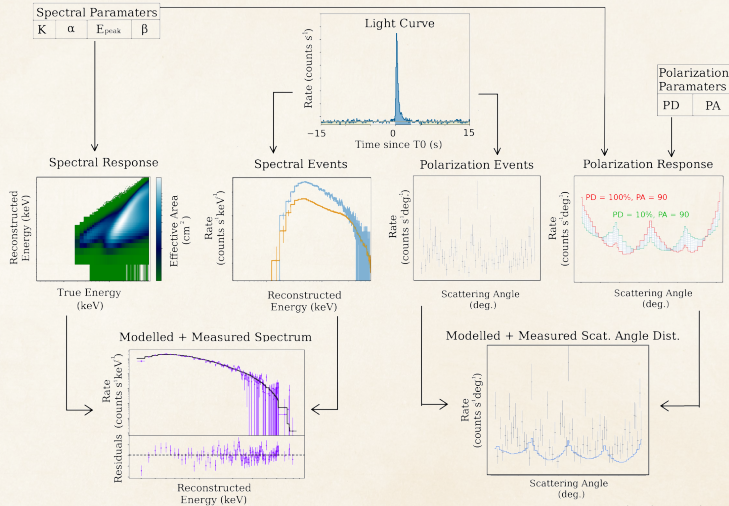
- Typical measured light and modulation curves shown below, complex modulation curve structure due to well-understood instrumental/geometrical effects
- POLAR detected 55 GRBs in 6 months of operation, 14 of which had enough statistics to be analyzed → joint spectral/polarization analysis with Fermi-GBM or Swift-BAT data using 3ML spectral fitting framework (github.com/threeML) and development of a polarization fitting plugin (github.com/grburgess/polarpy)



A&A 644, A124 (2020)

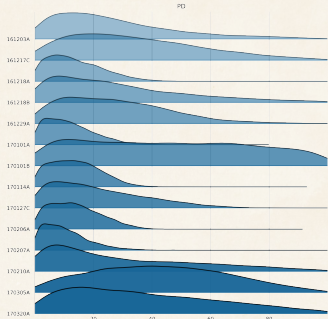
GRB Analysis Workflow

Spectral and polarization events are fitted in parallel using a forward folding method. The spectral part is jointly fitted with Fermi-GBM/Swift-BAT data.



POLAR GRB Polarization Results

- ★ Catalog of 14 GRBs analysed, results show a low or null polarization degree (excluding synchrotron emission models from toroidal magnetic field, compatible with photospheric emission model and other synchrotron models)
- ★ Time resolved analysis show a hint of quickly evolving polarization angle that washes out polarization degree on time integrated analysis
- ★ More statistics is needed in order to perform precise temporal and energy resolved analysis, with lowered energy threshold to probe emission models, and with bigger effective area and longer mission operation to get a larger catalog
→ **the POLAR-2 mission**



A&A 644, A124 (2020)

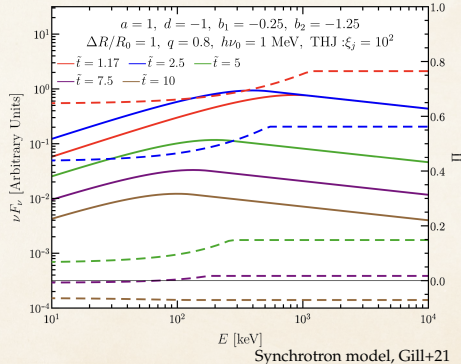
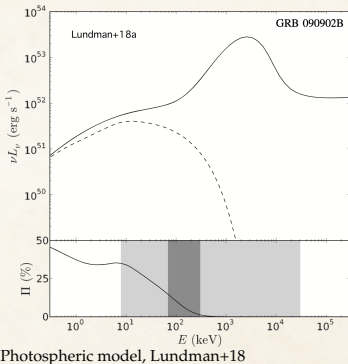


A&A 627, A105 (2019)

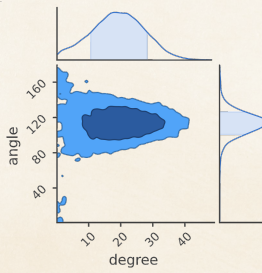
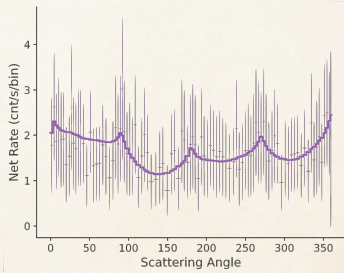
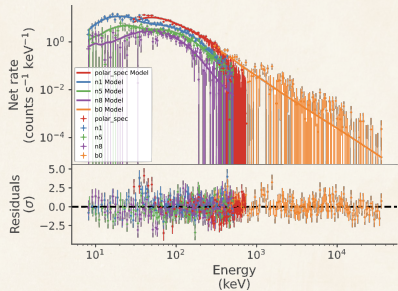
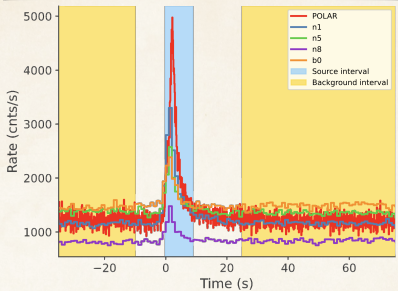
Theoretical Predictions

Energy Dependence of Polarization

- Energy-resolved polarimetric measurement made possible by increasing sensitivity of high energy polarimeters
- Theoretical models recently started to be extended to predict energy dependence of GRB prompt emission polarization



Energy integrated results: GRB170114A

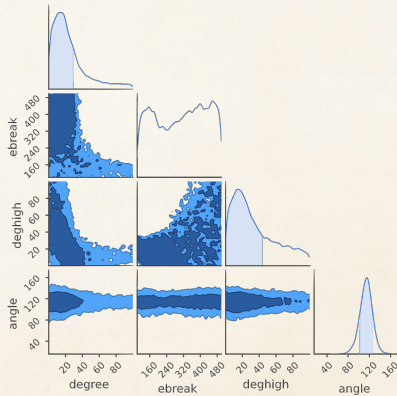


Energy resolved results: GRB170114A

Heaviside fit of the PD

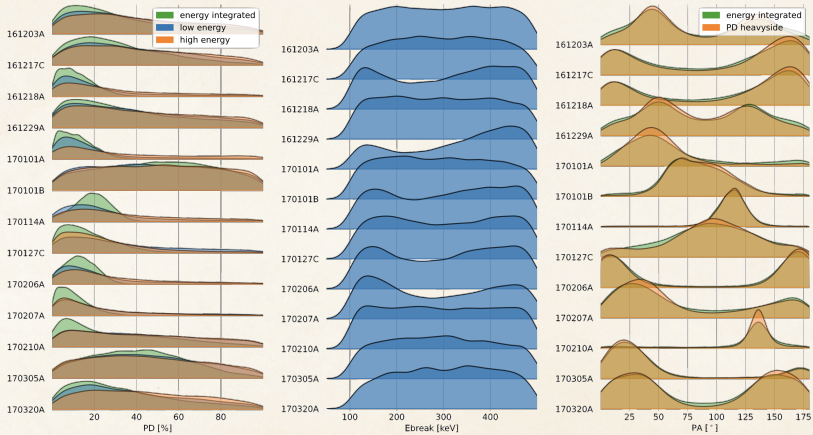
Fitting the PD using two energy bins (using complex functions is not possible due to limited statistics):

$$PD = \begin{cases} PD_{low} & \text{if } E < E_{break} \\ PD_{high} & \text{if } E > E_{break} \end{cases}; \quad PA = cst.$$



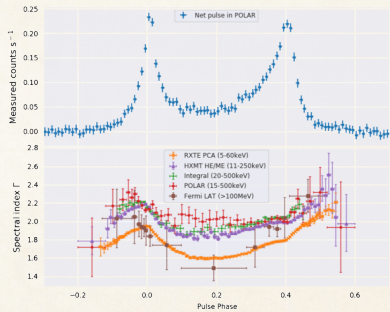
Energy resolved results: POLAR catalog

Heaviside fit of the PD



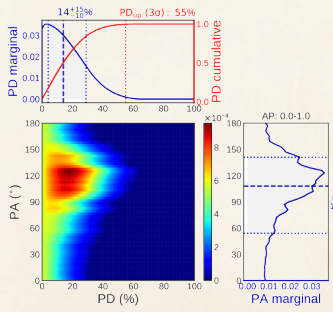
Crab pulsar results from POLAR

- Exposition of 400 h for spectral analysis, 1222 h for polarization analysis
- Nebula contribution subtracted, 3 pulse intervals studied: AP (0.0–1.0), P1 (0.0–0.2 || 0.8–1.0) and P2 (0.2–0.6)



Journal of High Energy Astrophysics 24 (2019) 15–22

	PD [%]	PA [°]
AP	$14^{+15}_{-10}\%$	$108^{+33}_{-54}\%$
P1	$17^{+18}_{-12}\%$	$174^{+39}_{-36}\%$
P2	$16^{+16}_{-11}\%$	$78^{+39}_{-30}\%$



MNRAS 512, 2827–2840 (2022)

What next ?

- POLAR was launched in September 2016 and operated for 6 months on-board TG-2
- It observed 55 GRBs, 2 pulsars, and some Solar Flares
- The polarimetric analysis of the 14 brightest GRBs shown low levels of polarization of the prompt emission
- Time-resolved analysis of single pulse GRBs shown a hint for time evolving PA within the pulse, washing out the PD on integrated analysis
- No significant energy dependence of the polarization parameters was observed with the POLAR data
- Higher quality measurements are needed for time and energy resolved polarization analysis: **POLAR-2**

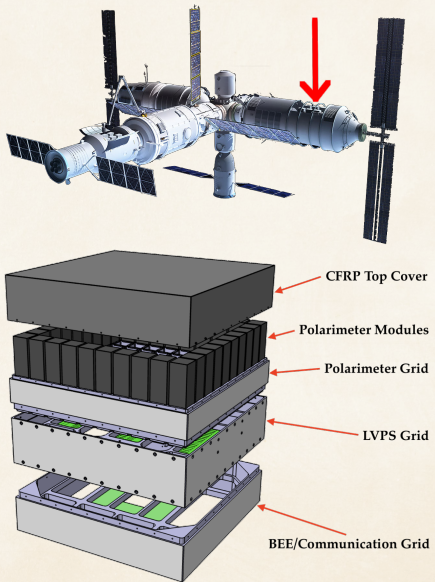


Section 3

Future of GRB Polarimetry with the POLAR-2 Mission

The POLAR-2 instrument

- ◆ Large scale GRB polarimeter based on POLAR's legacy
- ◆ 4 times bigger than POLAR (from 25 to 100 polarimeter modules), 10 times more sensitive (thanks to an improved design)
- ◆ Lowered energy threshold down to a few keV
- ◆ Two other payloads (low energy polarimeter and spectral imager) being developed
- ◆ Planned for a launch to the CSS



The POLAR-2 collaboration

About 20 people working on POLAR-2 from 4 countries:

- ◆ UniGe (DPNC), Switzerland: Management, polarimeter modules, instrument thermal and mechanical integration
- ◆ UniGe (DA), Switzerland: Online software system
- ◆ NCBJ, Poland: Back-End Electronics, Power Supply
- ◆ IHEP, China: Flight Model Acceptance, Spectrometers
- ◆ MPE, Germany: Qualification & Verification, Spectrometers



More information: <https://www.unige.ch/dpnc/polar-2>.



Narodowe Centrum Badań Jądrowych
National Centre for Nuclear Research
SWIERK

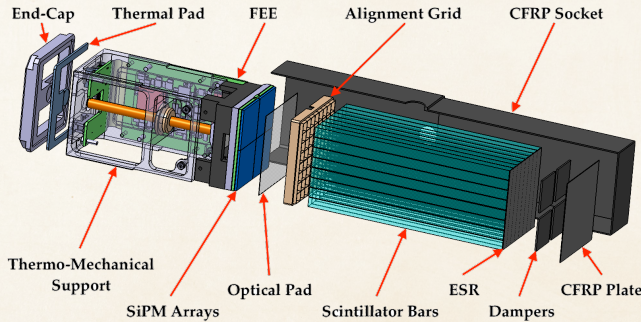


Max-Planck-Institut für
extraterrestrische Physik

Polarimeter Module Design

A polarimeter module consists of an 8×8 array of individually wrapped plastic scintillator bars read out by SiPM arrays. The optical efficiency of the module has been greatly improved thanks to several upgrades:

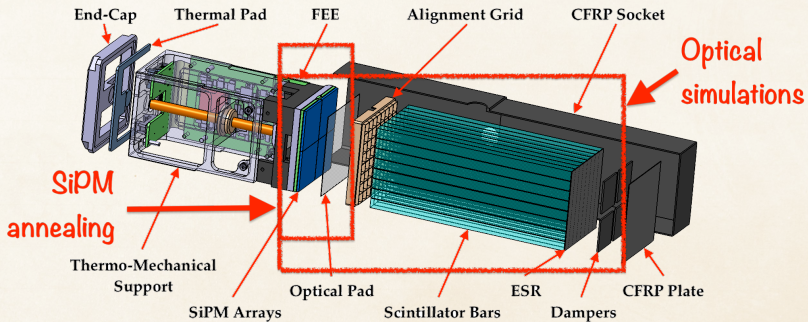
- ◆ SiPMs instead of MA-PMTs: peak PDE increased from 0.2 to 0.5
- ◆ Scintillators reshaped: shorter (better SNR), wider (less dead volume), non-truncated (thanks to very thin mechanical grid, better light yield)
- ◆ Improved wrapping, thinner optical coupling pad: crosstalk reduced by an order of magnitude



Polarimeter Module Design

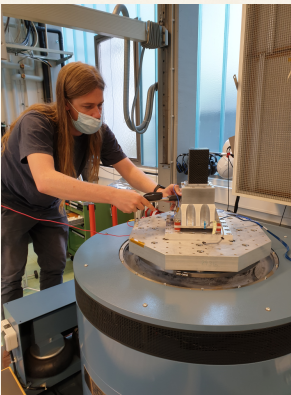
A polarimeter module consists of an 8×8 array of individually wrapped plastic scintillator bars read out by SiPM arrays. The optical efficiency of the module has been greatly improved thanks to several upgrades:

- ◆ SiPMs instead of MA-PMTs: peak PDE increased from 0.2 to 0.5
- ◆ Scintillators reshaped: shorter (better SNR), wider (less dead volume), non-truncated (thanks to very thin mechanical grid, better light yield)
- ◆ Improved wrapping, thinner optical coupling pad: crosstalk reduced by an order of magnitude



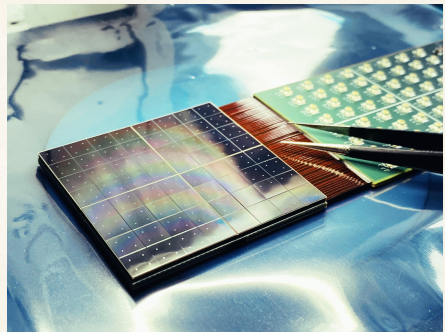
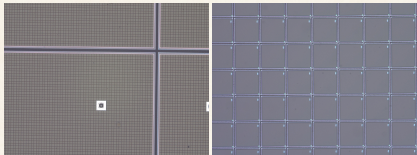
POLAR-2 Space Qualification

Many component- and module-level space qualification tests: thermal vacuum cycling, vibration and shock tests, irradiation campaigns etc.

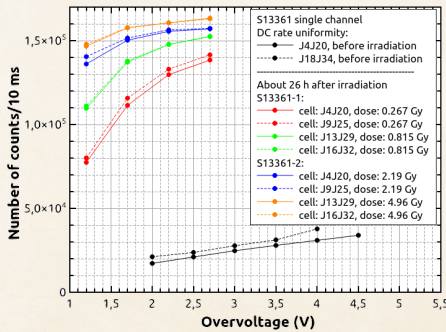


Silicon Photo-Multipliers Radiation Damage

Radiation damages SiPMs by inducing defects in the silicon lattice, leading to a higher DCR and dark current

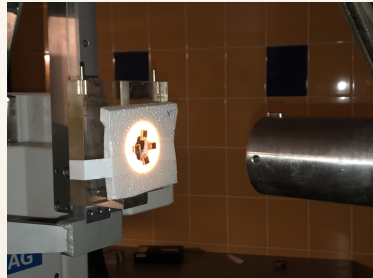


(Credit: Hybrid SA, POLAR-2 collab.)

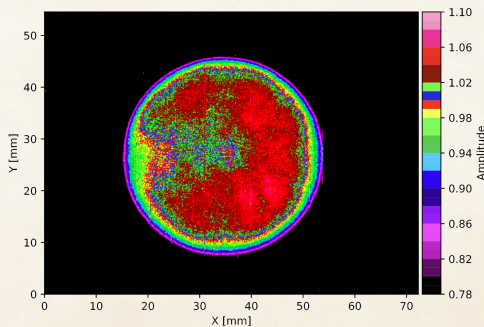


Exp. Astron. 55, p343–371 (2023)

SiPM Thermal Annealing Probe Station Setup

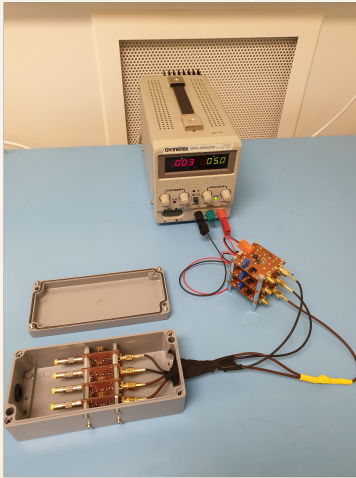
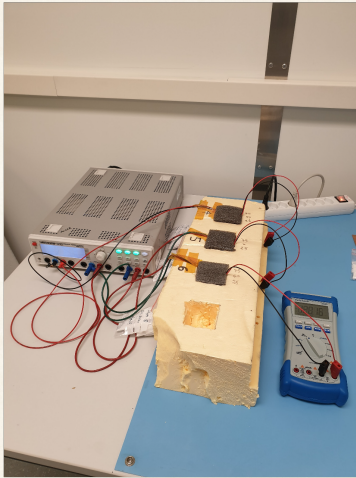


- ◆ NIM A 1048 (2023) 167934
- ◆ 58 MeV proton beam @IFJ-PAN, Krakow
- ◆ Sensors exposed to 0.134 Gy (equivalent to 1.7 yrs on the CSS according to Geant4 simulations)
- ◆ Fluence of 10^8 p/cm²



SiPM Thermal Annealing Sensors Storage Setups

- ◆ 21 S13360-60xx SiPMs from Hamamatsu (25, 50, and 75 μm) stored at 6 temperatures ranging from $-22.8 \pm 1.8^\circ\text{C}$ to $48.7 \pm 3.3^\circ\text{C}$
- ◆ 4 of the sensors are stored with a bias ($\Delta V = 3, 8, 12$ V)



SiPM Thermal Annealing Probe Station Setup

Vacuum control
for positioners
and chuck

Positioners
and probes

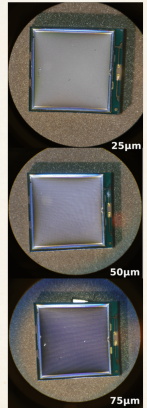
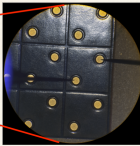
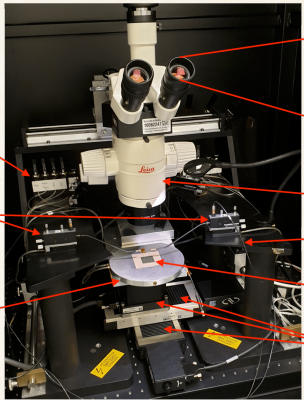
Chuck

Microscope

to HV power supply

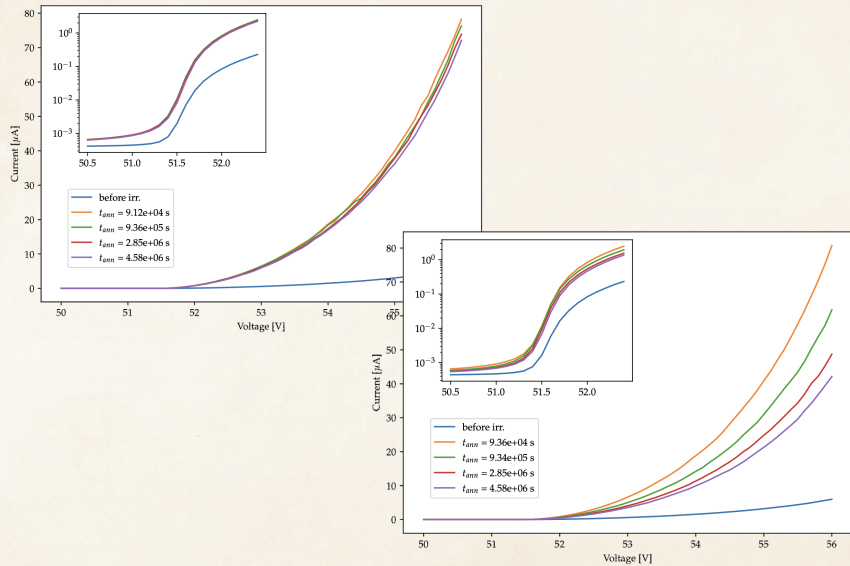
SiPM chip

x, y and z motors

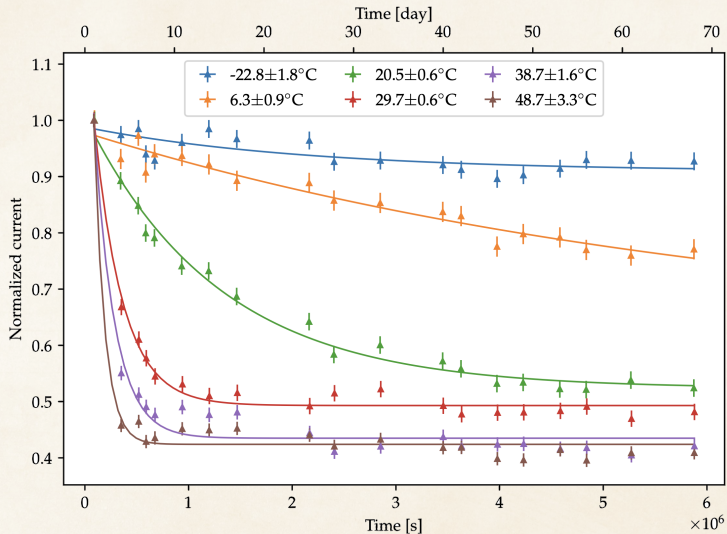


I-V measurement versus time

S13360-6075PE, $-22.8 \pm 1.8^\circ\text{C}$ vs. $20.5 \pm 0.6^\circ\text{C}$

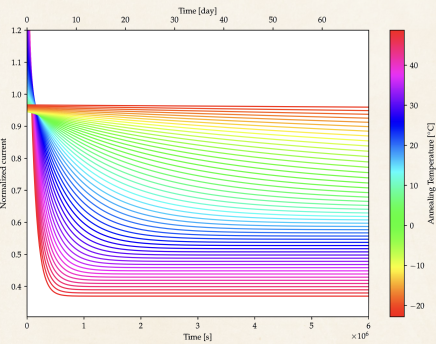
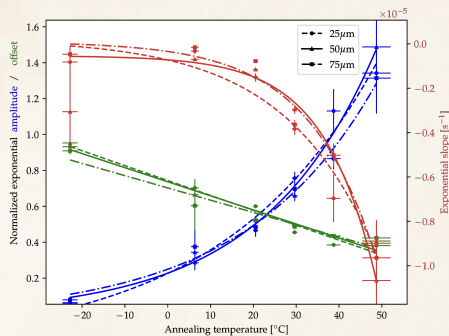


Time evolution of dark current at $\Delta V=3$ V 75 μm microcells



Exponential decay parameters vs. T_{annealing}

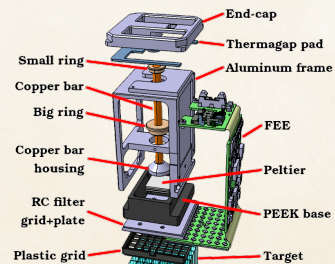
$$a(T) \times \exp(b(T) \cdot t) + c(T)$$



Annealing strategies for POLAR-2

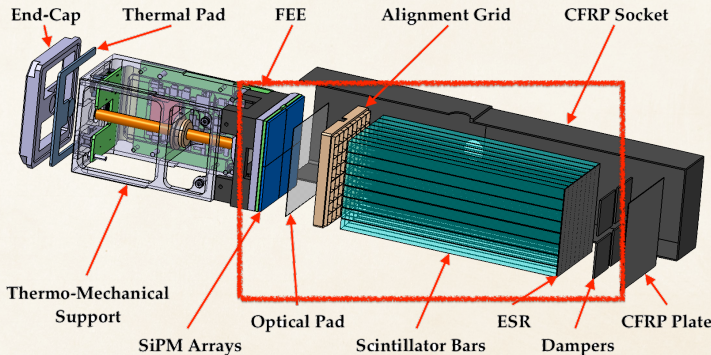
- ◆ SiPMs are being operated as cold as possible during scientific data taking thanks to a Peltier based active cooling system
- ◆ About once a year, the sensors can be annealed for a couple of days using power resistors (1.98 W @ 9 V) mounted on the back of the PCB
- ◆ Without annealing, the DCR is expected to increase by a factor 5 per year. This corresponds to an energy threshold increase of 0.75 keV for a SiPM intrinsic crosstalk of 10%. This number is halved with 1 day of annealing at 50°C every year.

Operating temperature [°C]	-10	0	20
Scenario 1 "No Annealing"	25µm	15.7 ± 0.8	
	50µm	15.4 ± 2.2	
	75µm	7.2 ± 0.9	
Scenario 2 "Continuous annealing"	25µm	13.15 ± 0.73	11.93 ± 0.67
	50µm	12.74 ± 1.84	11.61 ± 1.67
	75µm	5.80 ± 0.72	5.36 ± 0.65
Scenario 3a (1 day) "Continuous + Stimulated annealing"	25µm	8.02 ± 0.45	7.27 ± 0.41
	50µm	7.40 ± 1.07	6.75 ± 0.97
	75µm	3.59 ± 0.45	3.31 ± 0.40



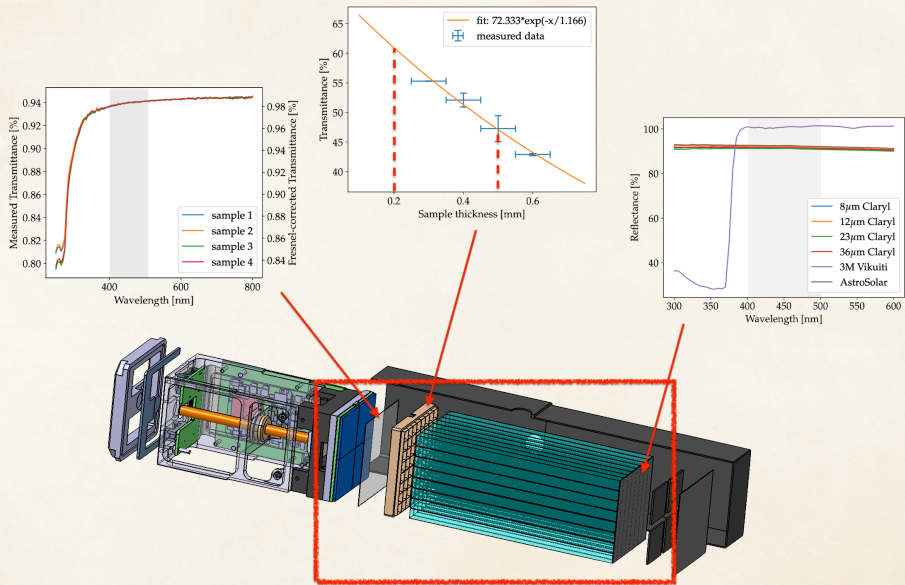
Motivation Behind Optical Characterization

- ◆ γ -rays gets converted into optical light in the scintillators, which gets collected by the SiPMs and converted into a measurable electrical signal pre-processed by the FEE
- ◆ The polarimeter module is therefore an optical system, and characterizing/simulation its optical behavior is crucial to understand/optimize the instrument performances



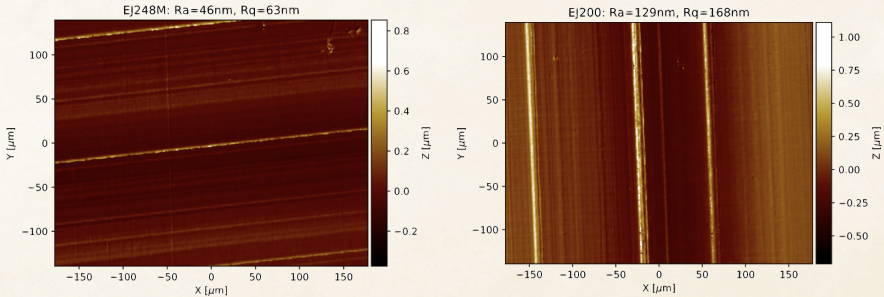
Optical Characterization

Reflectance and Transmittance measurements

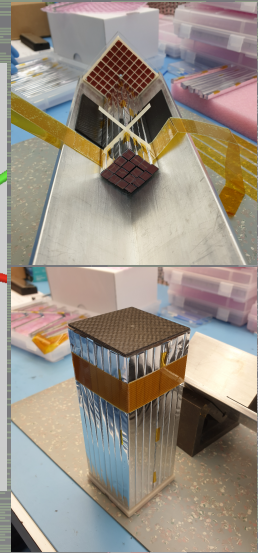
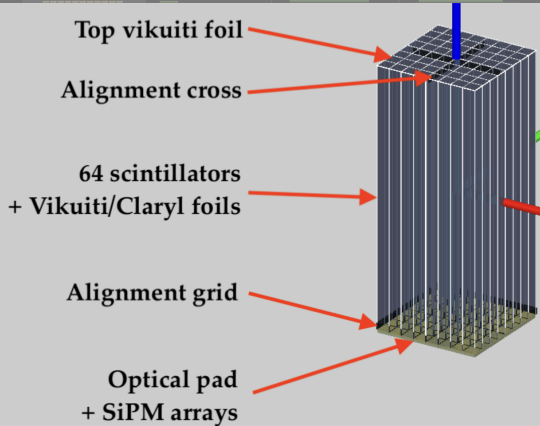


Plastic Scintillator Surface Roughness

- 2 types of plastic scintillators investigated for the polarimeter: EJ-200 (10'000 photons/1 MeV e^-) and EJ-248M (9'200 photons/1 MeV e^-) from Eljen
- Module light yield is higher with EJ-248M!! Our guess: EJ-200 is slightly softer, more light loss at the interface due to rougher surface
- Surface quality measured for both scintillators at HEPIA using an Interferometric Optical Microscope



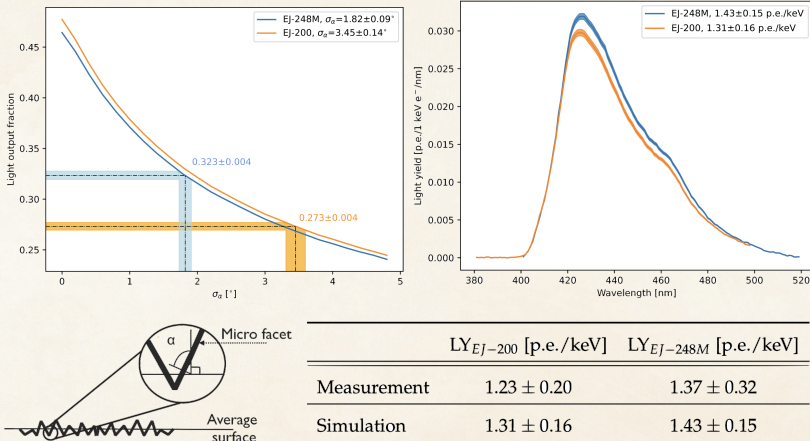
Geant4 Optical simulations



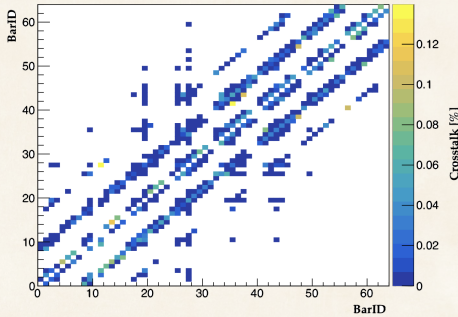
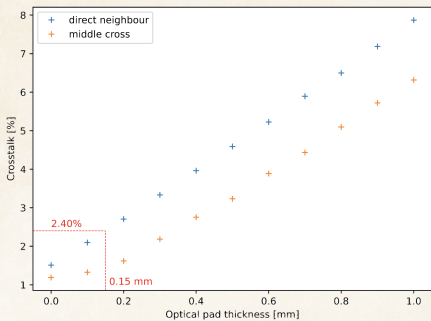
Polarimeter Module Light Yield

Optical Simulations vs. Measurements

- Great improvement compared to the 0.3 p.e./keV light yield in POLAR
- Allows to lower the energy threshold down to a few keV, significantly improves the statistics for a typical GRB spectrum



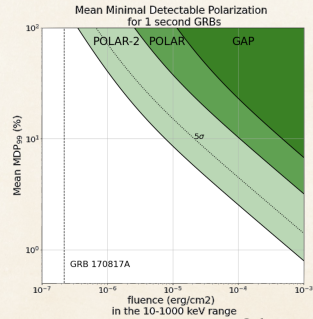
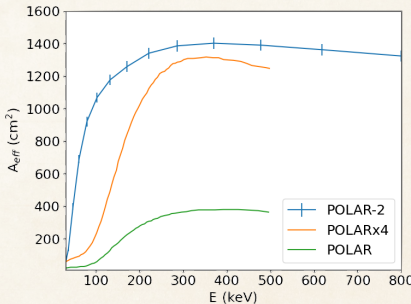
Applied Radiation and Isotopes 103 (2015) 15–24



- Measurement compatible with simulations: $P_{XT}=2.63 \pm 2.10\%$
- Compatible with expectation from simple calculation:
 $3 \text{ mm}/125 \text{ mm} \times 60.9\% = 1.46\% \times 47.1\% = 1.13\%$ for middle cross)
- Optical crosstalk was $\sim 15\%$ in POLAR: huge improvement thanks to the new wrapping technique and thinner SiPM entrance resin/opt. pad
- The improvement in optical crosstalk leads to a better sensitivity to polarization
- More details in [DOI:10.1088/1748-0221/20/02/P02010](https://doi.org/10.1088/1748-0221/20/02/P02010)

Anticipated Science Performances

- ◆ Effective area greatly increased, especially at low energies, thanks to the improved module light yield
- ◆ Improvement of the modulation factor μ_{100} (sensitivity to polarization) compared to POLAR
- ◆ About 50 GRBs/year with quality equal or higher than the best POLAR measurements (**fast alerts** sent to ground, possibly joint GW observation)
- ◆ POLAR-2 is sensitive to lower levels of polarization for weaker GRBs



Galaxies 2021, 9, 82.

$$MDP = \frac{4.29}{\mu \cdot R} \cdot \sqrt{\frac{R + B}{T}}$$

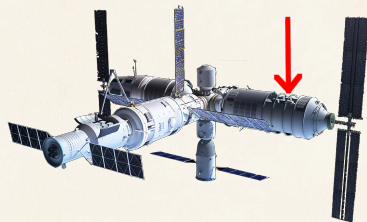
(Weisskopf+ 2010, SPIE, Strohmayer & Kallman 2013, ApJ)

Enhanced POLAR-2: LPD and BSD

Two other payloads proposed to the China Space Station (CSS):

X-ray Polarimeter (LPD) lead by GuangXi University, Nanning

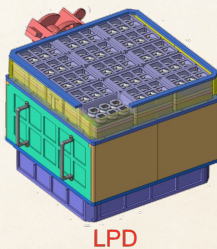
& Broad-band Spectrometer (BSD) lead by IHEP, Beijing



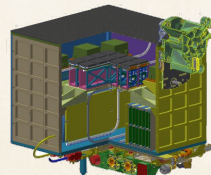
➤ **Low-energy Polarization Detector:**

LPD

- ~2-10 keV X-ray polarimetry
- **Broad energy-band Spectrum Detector: BSD**
- ~10-2000keV
- Accurate GRB localization and spectroscopy for HPD and LPD
- **Status: Selected, to be adopted**

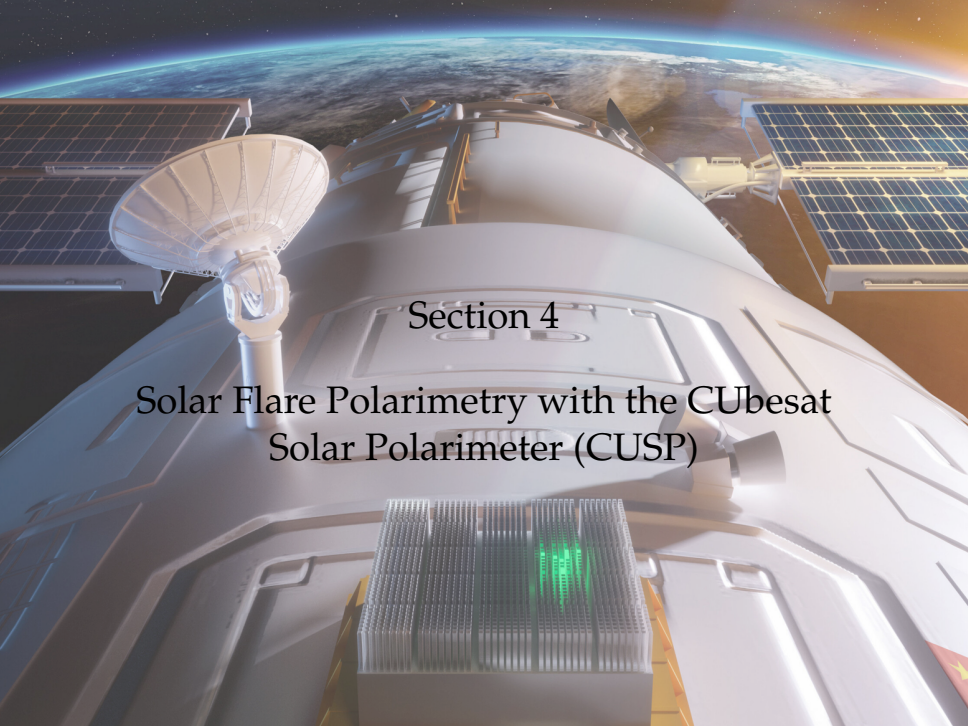


LPD



BSD

from Jianchao Sun, IHEP

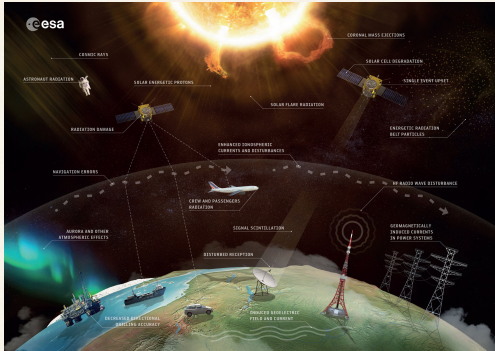


Section 4

Solar Flare Polarimetry with the CUbesat Solar Polarimeter (CUSP)

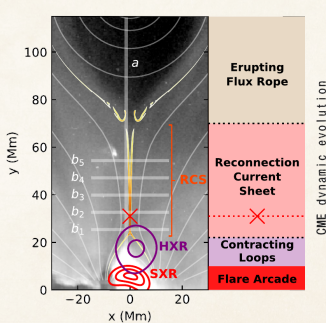
Heliophysics and Space Weather

- Solar activity, including **Solar flares (SFs)**, can be disruptive for human technological activities in space and on ground
 - The occurrence of SFs is very often associated to **Coronal Mass Ejection (CME)** and **Solar Energetic Particle (SEPs)** events on the ground
 - SF **can also occur** alone producing a **direct acceleration** of particles towards the Earth

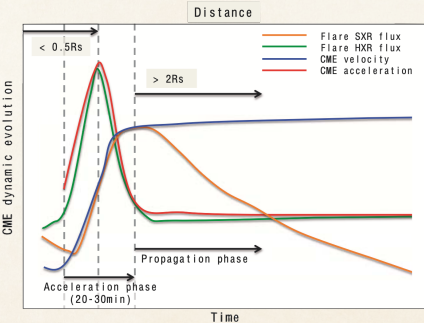


Solar Flares: CME feedback

- ⌚ Most powerful eruptions associated to powerful flares
- ⌚ HXRs are related to CME acceleration \Rightarrow **HXR polarimetry** could improve the knowledge of the **initial conditions** of the eruption of most powerful CME
- ⌚ SXRs are related to CME velocity
- ⌚ The rapid CME development in the lower corona during the acceleration phase strongly correlates with the associated flare activity.



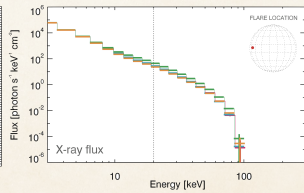
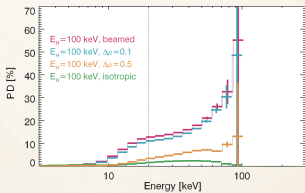
Chen B. et al. (2020), Nat. Astron.



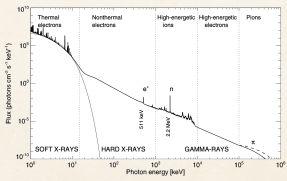
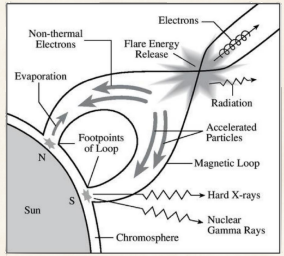
Temmer (2016), Astron. Nachr.

Motivation for X-ray Polarimetry of SFs

- ◆ SFs originate from **magnetic reconnection** in loop structures in solar corona
- ◆ SFs energy spectrum in the X-rays is dominated by:
 - thermal Bremsstrahlung (due to plasma heating, expected weakly polarized by Emslie&Brown 1980) + emission lines < 10 keV
 - non-thermal Bremsstrahlung (at the loop top and footprints, due to particle acceleration along magnetic field lines) expected highly polarized [Zharkova+ 2010] >10-20 keV
- ◆ (Linear) X-ray polarimetry would allow to **disentangle degeneracies** in models of particle beaming and magnetic field structure (also without imaging of the SF)



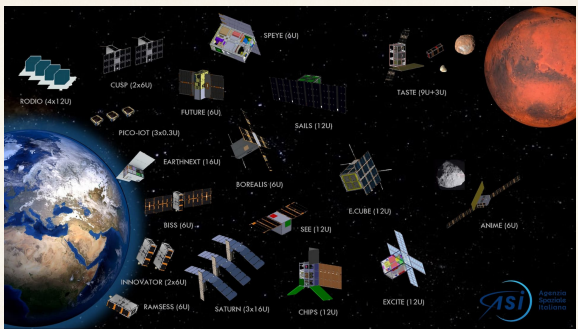
Jeffrey+ 2020 (A&A)



Aschwanden (2005)

The Project Framework

- The Italian Space Agency (ASI) started a new national program named Alcor for funding the development of CubeSat technologies and missions
- CUSP is one of the 20 selected missions among 49 proposals
- 22 participants from Research Institutes and Universities and 78 companies, mainly Small and medium-sized ones

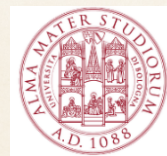


The CUSP Collaboration

- ◆ **INAF: IAPS-Roma:** Prime contractor, PI-ship, and Payload; **OAS-Bologna:** Detector Simulation; **OAR-Roma:** Lab SW Support
- ◆ **IMT s.r.l.:** Satellite Platform
- ◆ **SCAI Connect s.r.l.:** Payload Electronics
- ◆ **Università di Bologna – CIRI AERO:** Mission Analysis
- ◆ **Università della Tuscia:** Ground Segment
- ◆ **Italian Space Agency (ASI):** Project Control

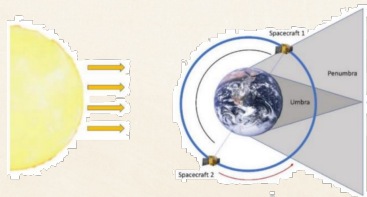
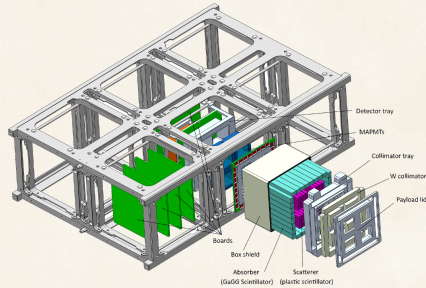


Website: <https://www.iaps.inaf.it/it/missioni-spaziali/cusp>.



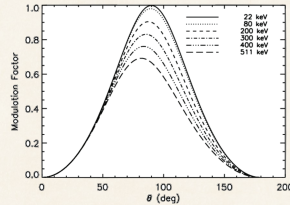
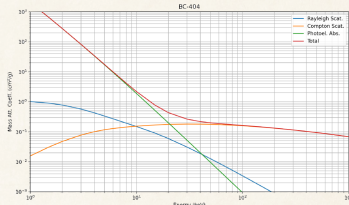
The CUSP Payload

- ◆ Constellation of two 6U CubeSats orbiting the Earth on SSO orbit (500-600 km) to observe the Sun
- ◆ Monitoring of the Sun with a time fraction >68% during the 3 years nominal life-time
- ◆ X-ray polarimetry of Solar Flares in the 25-100 keV energy band
- ◆ Each satellite hosts a **dual-phase Compton scattering polarimeter** that exploits **coincidence** measurements between plastic (scatterer) and inorganic (absorber) scintillator rods
- ◆ **1 RPM rotation** of the spacecraft around the polarimeter symmetry axis pointing the Sun allows to reduce the systematic effect known as spurious polarization



Dual Phase Design

- ➊ High probability of **scattering in plastic** material (4 MAPMTs read out with a MAROC-3A ASIC by WEEROC)
- ➋ 90° scattering produces maximum modulation of the signal
- ➌ @20 keV only 750 eV of Compton energy deposit for scattering at 90° , PMT needed (1-3 optical photons to collect)



NIST XCOM

Fabiani & Muleri 2014

- ➊ High probability of **photoelectric absorption** in the absorber (GAGG) material (32 APDs read out with a SKIROC-2A ASIC by WEEROC)
- ➋ Measurement of **coincidences** Scatterer/Absorber allows effective **background reduction**
- ➌ **Fast schedule, no R&D possible**, we need heritage and space proven items as much as possible. We selected APDs from past TSUBAME mission unfortunately lost in 2015 (and similar MAPMTs) by Hamamatsu (Japan - Yoichi Yatsu 2014, SPIE Proc.)

Polarimetric Sensitivity

- Minimum Detectable Polarization (Weisskopf+ 2010, SPIE, Strohmayer & Kallman 2013, ApJ) in the 25-100 keV energy band (CBE based on benchmark SFs from Saint-Hilaire et al. (2008), Sol. Phys. 250, 53–73)

Flare Class	Integration time (s)	MDP (%) (25-100 keV)
M5.2	284	10.2
X1.2	240	5.0
X10	351	1.1

$$MDP = \frac{4.29}{\mu \cdot R} \cdot \sqrt{\frac{R + B}{T}}$$

$$Q = \mu \sqrt{\varepsilon}$$

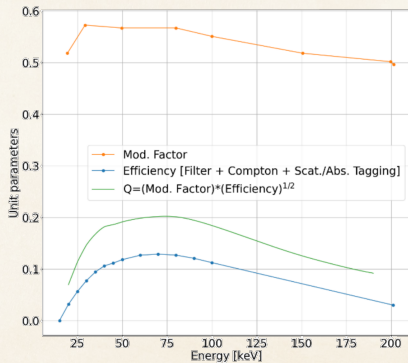
R: source rate

B: background rate

T: integration time

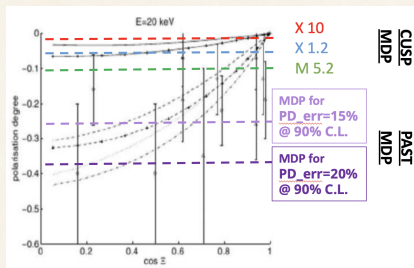
μ : modulation factor

ε : quantum efficiency



Polarimetric Sensitivity

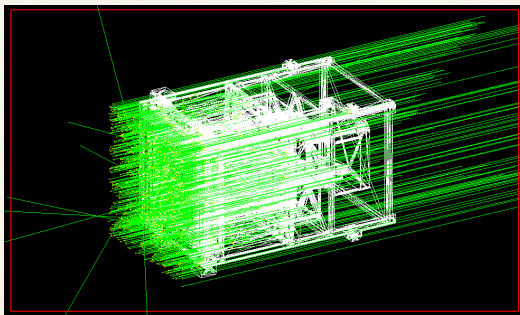
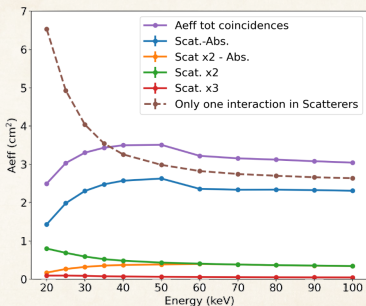
- ⌚ MDP $\sim 3\sigma$ for 1 parameter measurement
(Strohmayer & Kallman 2013, ApJ)
- ⌚ PD errors of about:
 - 15% with a C.L. of 90% ($\sim 1.645\sigma$) correspond to an MDP $\sim 27\%$
 - 20% corresponds to an MDP $\sim 37\%$
- ⌚ CUSP will reduce significantly the MDP wrt past observations.
- ⌚ Flares are expected to be polarized at tens of %, few minutes of integration time allow to measure with high significance their polarization



Zharkova+ 2010 (A&A)

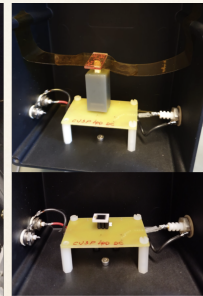
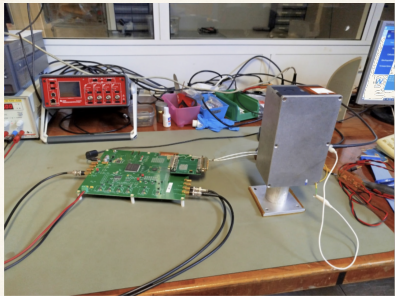
Design Optimization: Geant4 Simulations

- ⌚ Analysis of the **effective area** (A_{eff}) in progress for design and analysis optimization
- ⌚ We are currently working on getting the **spurious modulation** and **modulation factor**



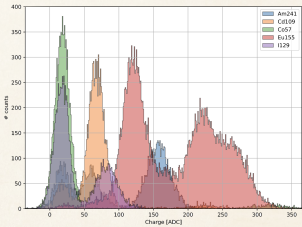
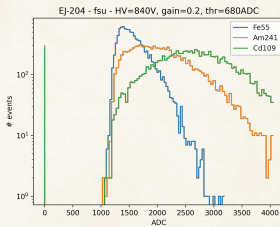
Laboratory Test of the Acquisition Chains

- ⌚ CUSP is employing **2 acquisition chains** for the **Absorbers** (GAGG + APD + SKIROC-2A) and **Scatterers** (Plastic + MA-PMTs + MAROC-3A)
- ⌚ Preliminary tests are being conducted based on ASIC Test Boards (WEEROC) and single scintillator bars coupled to sensors



Single Channel Energy Calibration

- ⌚ CUSP is employing **2 acquisition chains** for the **Absorbers** (GAGG + APD + SKIROC-2A) and **Scatterers** (Plastic + MA-PMTs + MAROC-3A)
- ⌚ Preliminary tests are being conducted based on ASIC Test Boards (WEEROC) and single scintillator bars coupled to sensors
- ⌚ Measuring preliminary performances: energy range, noise optimization and energy threshold, noise rejection with coincidences between the two systems

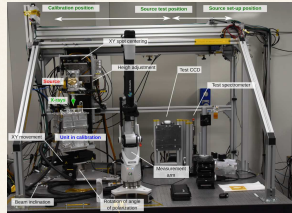


Impinging Energy (keV)	Scattering angle (deg)	Compton energy deposit (keV)
20	90	0.753
25	90	1.17
30	90	1.66
40	90	2.90
50	90	4.46
60	90	6.31
80	90	10.8
100	90	16.4
	65	10.2

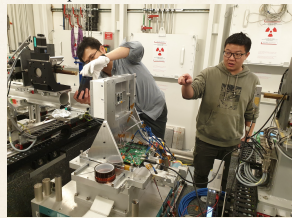
- ⌚ Next step is to test the two scintillators in **coincidence** to measure Compton events

Payload Calibration Plan

- ◆ Currently using **calibration sources** (Fe55 – 5.9keV, Cd109 – 22 and 88 keV, Am241 – 59.5 keV, Co57 – 123 keV) with single channel absorber/scatterer read out by ASIC development boards provided by WEEROC
- ◆ Soon building a reduced version of the instrument with **4×4 scatterers surrounded by 16 absorbers** to be read out by a **custom FEE** embedding both ASICs and an FPGA to apply the coincidence trigger logic
- ◆ This reduced module will be **calibrated in-house using calibration facilities** developed for IXPE's GPD calibration based on X-ray tubes combined with Bragg diffraction crystals to get a highly polarized X-ray flux
- ◆ Possibility of **calibration at ESRF** (Grenoble, France) with synchrotron polarized beam in the 20-500 keV range, such beam line has already been used for calibration of POLAR as well as prototypes modules from POLAR-2 HPD and BSD



ICE setup @INAF-IAPS

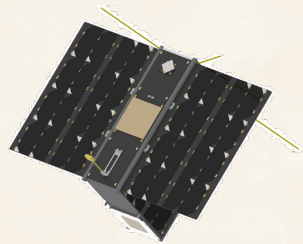


POLAR-2 ESRF beam test

The Satellite Platform

- Designed and produced by **IMT s.r.l.** company
- **6U CubeSat** platform based on the heritage of the HORTA and EOSS platforms (funded by Italian regional POR / FESR 2014-20 projects of Lazio and Puglia regions, respectively).

Peak Power	~ 30 W with Deployable Panels in Sun Pointing
Battery	Up to 84 Wh (baseline 42 Wh)
Pointing accuracy	$\pm 2^\circ @ 1\sigma$
Operative frequencies	S-Band downlink; UHF-Band uplink / downlink
Downlink throughput	Up to 5 Mbps
Available interfaces	CAN Bus, I2C, UART, SPI, RS485
Regulated bus	3.3V, 5V e 12V
Not regulated bus	16V (12V-16.8V)
Available volume for the payload	2.5U
Nominal life time	3 years in LEO



The Ground Station

- ⌚ Located on a building of the Università della Tuscia in Viterbo (Lazio, Italy)
- ⌚ Built in 2019 for the HORTA project (funds POR/FESR 2014-2020 by Lazio Region)
- ⌚ Available antennas and bands:
 - ⌚ VHF: Uplink and Downlink
 - ⌚ UHF: Uplink and Downlink
 - ⌚ S-band: Downlink
 - ⌚ UHF/VHF bandwidth:
 - Downlink: default 9.6 kbps
(available also 1.2 / 2.4 / 4.8 kbps)
 - Uplink: default 1.2 kbps
(available also 2.4 / 4.8 / 9.6 kbps)
- ⌚ S-band bandwidth:
 - Downlink: up to 1 Mbps

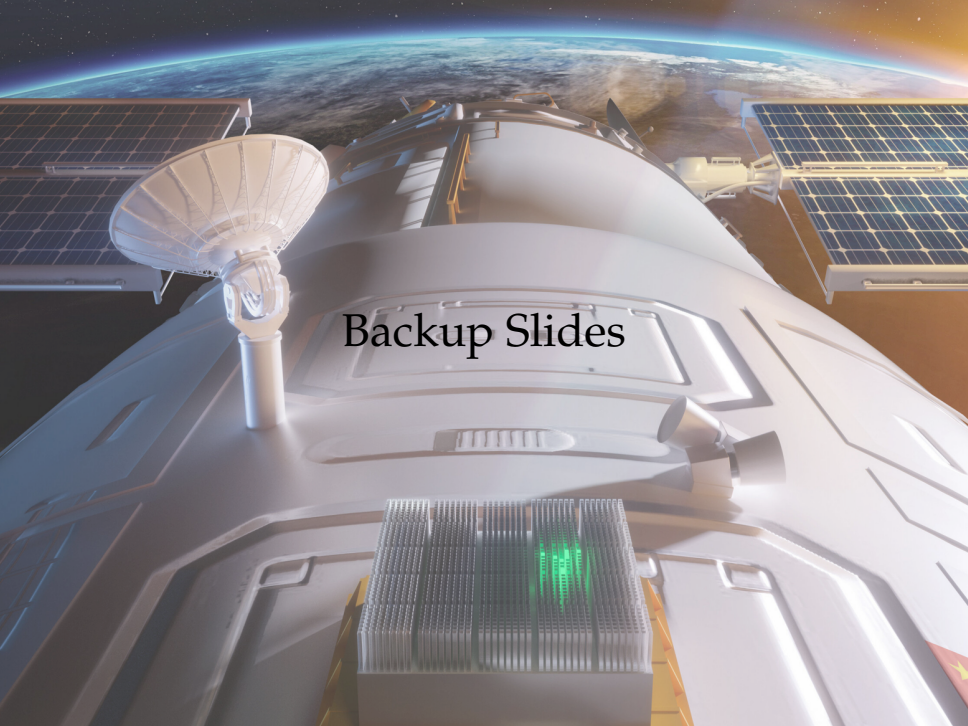


Project Status

- The 12 months Phase B started last December to define a preliminary design and deliver a representative prototype of the polarimeter
- Next step would be to propose a 15 months combined Phase C/D
- Model Philosophy:
 - 1 detector prototype at the end of Phase B. Representative of the detector front-end (from TRL 3 to TRL 4)
 - 1 payload sub-system Structural Model at the end of Phase B (scintillator bars holding system)
 - 1 payload EQM (design phase B, production and test phase C). Representative of the payload (from TRL 4 to TRL 7)
 - Trade-off assessment to allow ASI to decide if to continue with a 2 CubeSats constellation or with a single CubeSat. Depending on the outcome of the trade-off:
 - 1 Proto-flight Model (PFM). To qualify at proto-qualification level
 - 1 additional Flight Model (FM). To qualify at acceptance level
- Current launch window: late 2027/early 2028



Thank you!



Backup Slides

GRBs are usually spectrally described by a Band function (Band+93):

$$N_E(E) = \begin{cases} A \left(\frac{E}{100 \text{ keV}} \right)^\alpha e^{-E/E_0} & \text{if } (\alpha - \beta)E_0 \geq E; \\ A \left(\frac{(\alpha - \beta)E_0}{100 \text{ keV}} \right)^{\alpha - \beta} e^{\beta - \alpha} \left(\frac{E}{100 \text{ keV}} \right)^\beta & \text{if } (\alpha - \beta)E_0 \leq E. \end{cases}$$

Their spectrum can sometimes be better fitted with a Cut-off Power-Law (CPL) function:

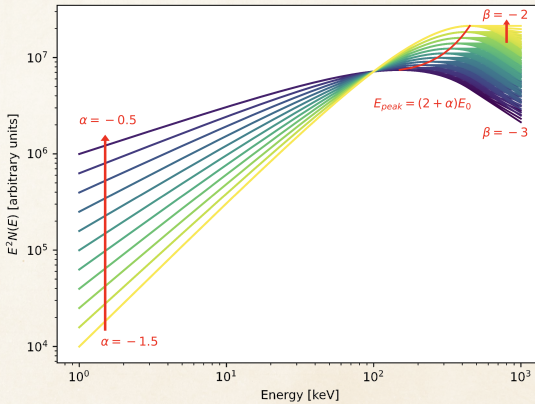
$$N_E(E) = K \left(\frac{E}{100 \text{ keV}} \right)^{-\alpha} e^{-E/E_c}$$

GRB Spectrum

The Band Function

GRBs are typically described by a non-thermal spectrum parameterized by the empirical Band function (smoothly joined broken power-laws):

$$N_E(E) = \begin{cases} A \left(\frac{E}{100 \text{ keV}} \right)^\alpha e^{-E/E_0} & \text{if } (\alpha - \beta)E_0 \geq E; \\ A \left(\frac{(\alpha - \beta)E_0}{100 \text{ keV}} \right)^{\alpha - \beta} e^{\beta - \alpha} \left(\frac{E}{100 \text{ keV}} \right)^\beta & \text{if } (\alpha - \beta)E_0 \leq E. \end{cases}$$



⊗ Top-Hat (uniform) Jet (THJ):

$$\frac{L'_{\nu'}(\theta)}{L'_{\nu',0}} = \frac{\Gamma(\theta)}{\Gamma_0} = \begin{cases} 1 & \text{if } \theta \leq \theta_j; \\ 0 & \text{if } \theta > \theta_j. \end{cases}$$

⊗ Smoothed Jet: Exponential and Power Law Wings ($\xi_j \equiv (\Gamma \theta_j)^2$)

$$\frac{L'_{\nu'}}{L'_{\nu',0}} = \begin{cases} 1 & \text{if } \xi \leq \xi_j; \\ \exp \left[\left(\sqrt{\xi_j} - \sqrt{\xi} \right) / \Delta \right] & \text{if } \xi > \xi_j. \end{cases} \quad \frac{L'_{\nu'}}{L'_{\nu',0}} = \begin{cases} 1 & \text{if } \xi \leq \xi_j; \\ \left(\frac{\xi}{\xi_j} \right)^{-\delta/2} & \text{if } \xi > \xi_j. \end{cases}$$

⊗ Truly structured Jet: Gaussian Jet (GJ)

$$\frac{L'_{\nu'}(\theta)}{L'_{\nu',0}} = \frac{\Gamma(\theta) - 1}{\Gamma_c - 1} \propto \exp \left(-\frac{\theta^2}{2\theta_c^2} \right)$$

⊗ Truly structured Jet: Power Law Jet (PLJ)

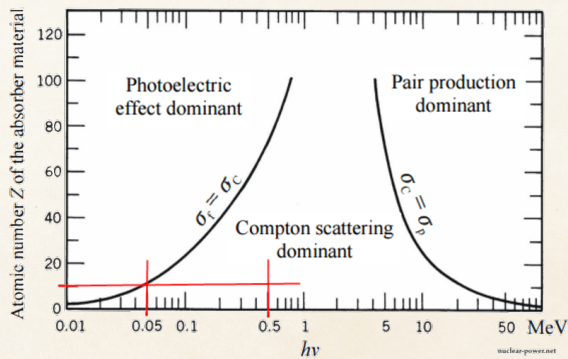
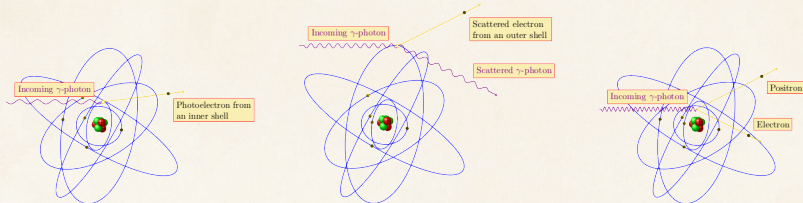
$$\frac{L'_{\nu'}(\theta)}{L'_{\nu',0}} = \Theta^{-a}, \quad \frac{\Gamma(\theta) - 1}{\Gamma_c - 1} = \Theta^{-b}, \quad \Theta \equiv \sqrt{1 + \left(\frac{\theta}{\theta_c} \right)^2}$$

$$\sigma \equiv \frac{w'_B}{w'_m} = \frac{B'^2}{4\pi \left(\rho' c^2 + \frac{\hat{\gamma}}{\hat{\gamma}-1} P' \right)}$$

- ⊗ $w'_B = B'^2 / 4\pi$ is the magnetic field enthalpy
- ⊗ $w'_m = \rho' c^2 + \frac{\hat{\gamma}}{\hat{\gamma}-1} P'$ is the matter enthalpy
- ⊗ Kinetic Energy Dominated (KED) flow: $\sigma < 1$
- ⊗ Poynting Flux Dominated (PFD) flow: $\sigma > 1$

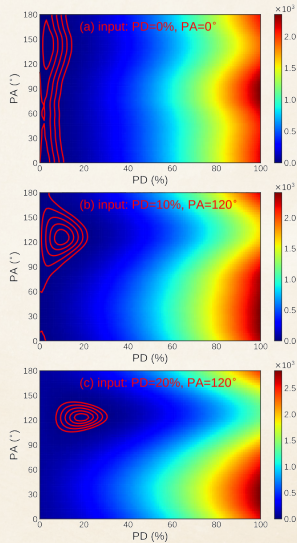
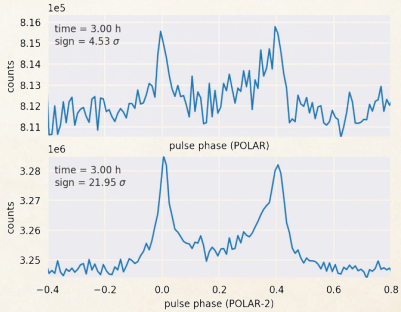
Low-Z scintillators

Optimized for Compton Scattering



Crab predictions for POLAR-2

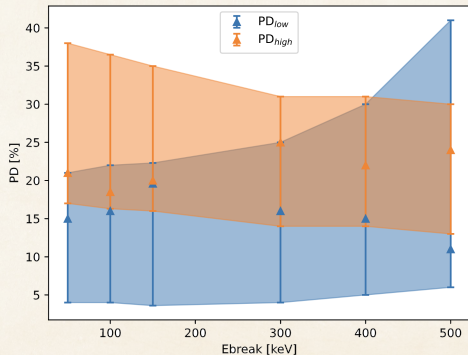
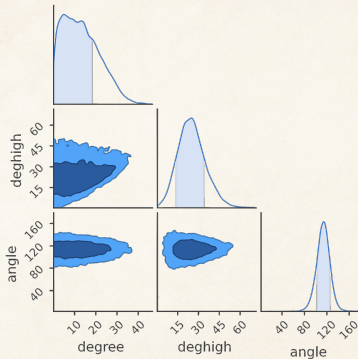
- ❖ POLAR spectral fitting: $\sim 400\text{h}$, $58.14\sigma \rightarrow$ will be achieved with 33h POLAR-2 exposure
- ❖ 2yrs of POLAR-2 data \implies more detailed spectral analysis of the Crab pulsar, and even of other PSRs (e.g. PSR B1509-58)
- ❖ If Crab pulsar is unpolarized: 5σ upper limits on the PD to a level of $\sim 20\%$. If Crab pulsar is 10 or 20% polarized, it will be confirmed with 5 or 4σ



Energy resolved results: GRB170114A

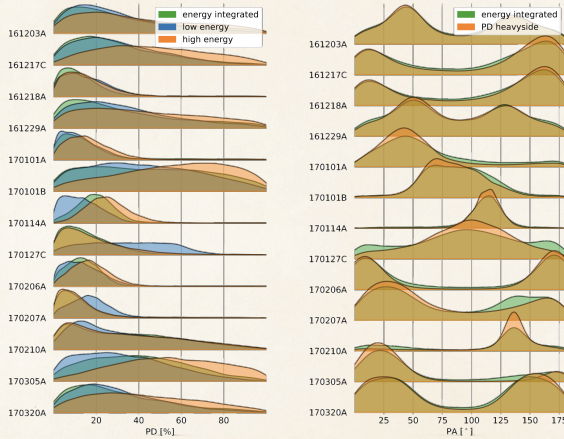
Heaviside fit of the PD, fixed break

$$PD = \begin{cases} PD_{low} & \text{if } E < 150 \text{ keV} \\ PD_{high} & \text{if } E > 150 \text{ keV} \end{cases}; \quad PA = cst.$$



Energy resolved results: POLAR catalog

Heaviside fit of the PD, $E_{break} = 150$ keV

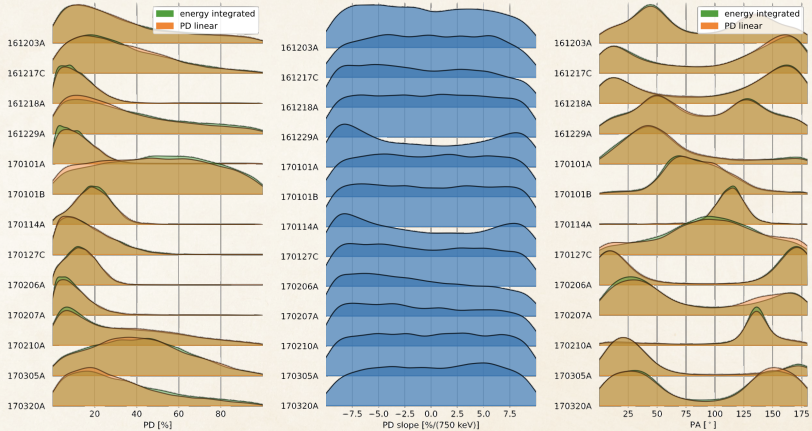


PD and PA were also fitted versus energy using a linear function, no significant energy dependence was found.

Energy resolved results: POLAR catalog

Linear fit of the PD

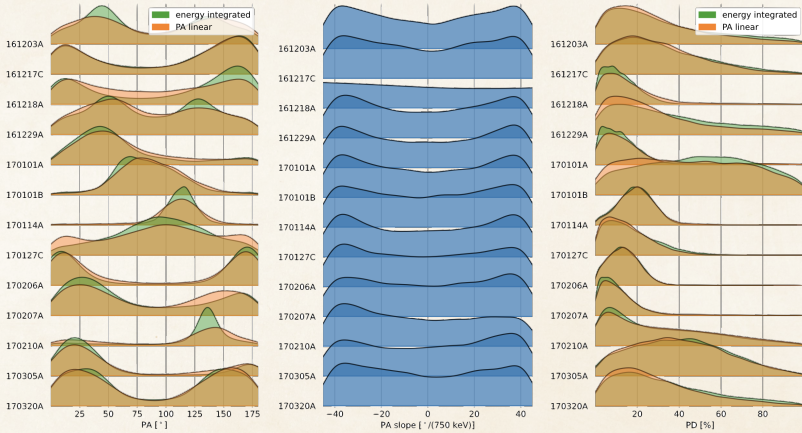
$$PD = PD_{intercept} + PD_{slope} \times \frac{E}{E_{max}} ; \quad E_{max} = 750 \text{ keV} ; \quad PA = cst.$$



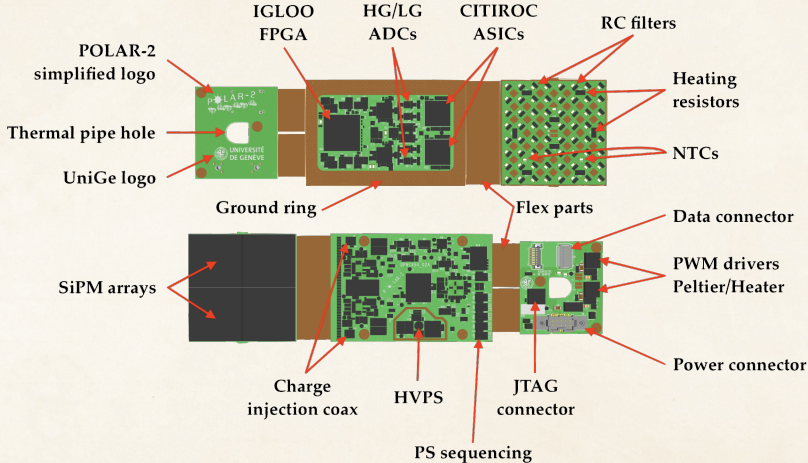
Energy resolved results: POLAR catalog

Linear fit of the PA

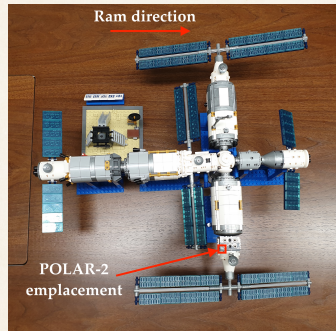
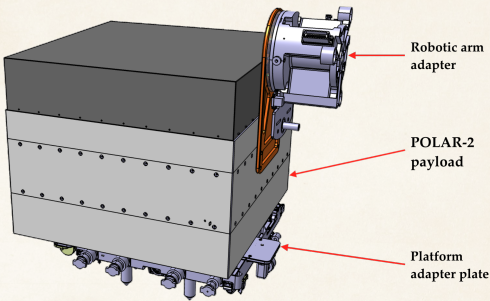
$$PA = PA_{intercept} + PA_{slope} \times \frac{E}{E_{max}} ; \quad E_{max} = 750 \text{ keV} ; \quad PD = cst.$$



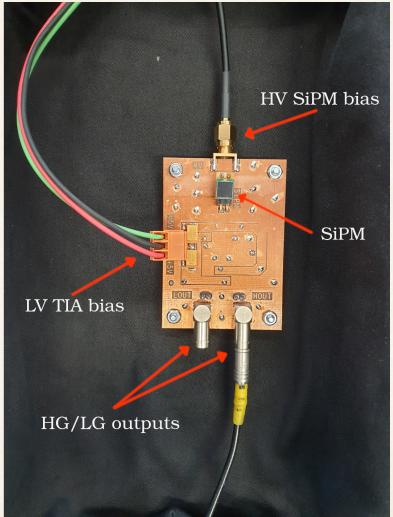
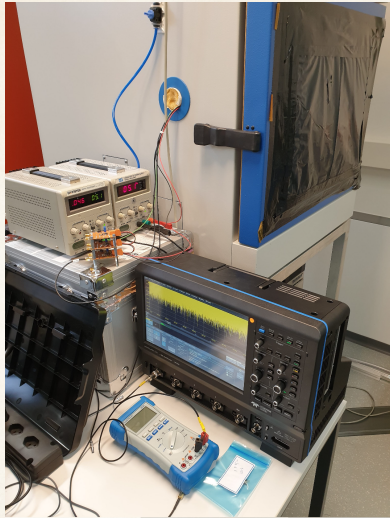
POLAR-2 Front-End Electronics



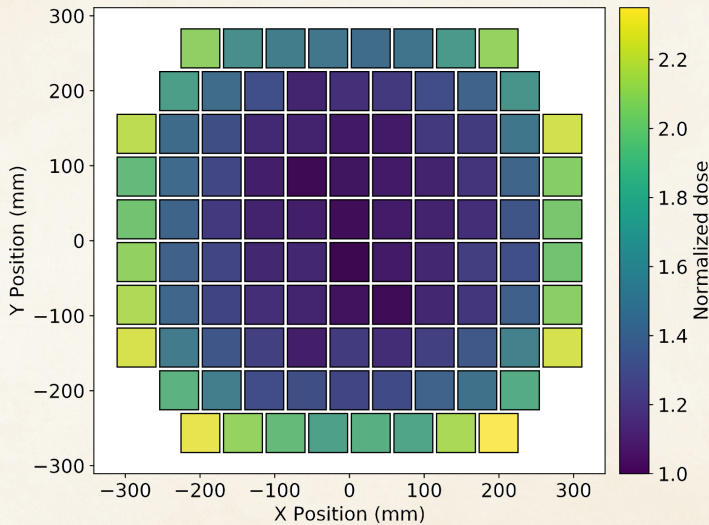
POLAR-2 Mounting on the CSS



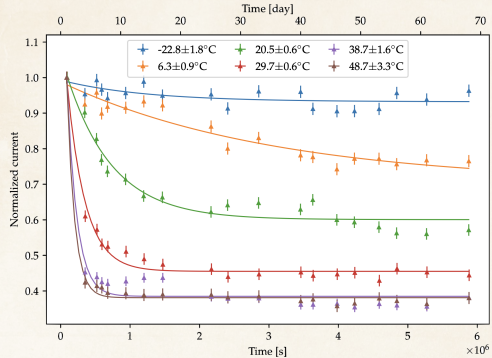
SiPM Thermal Annealing DCR Measurement Setup



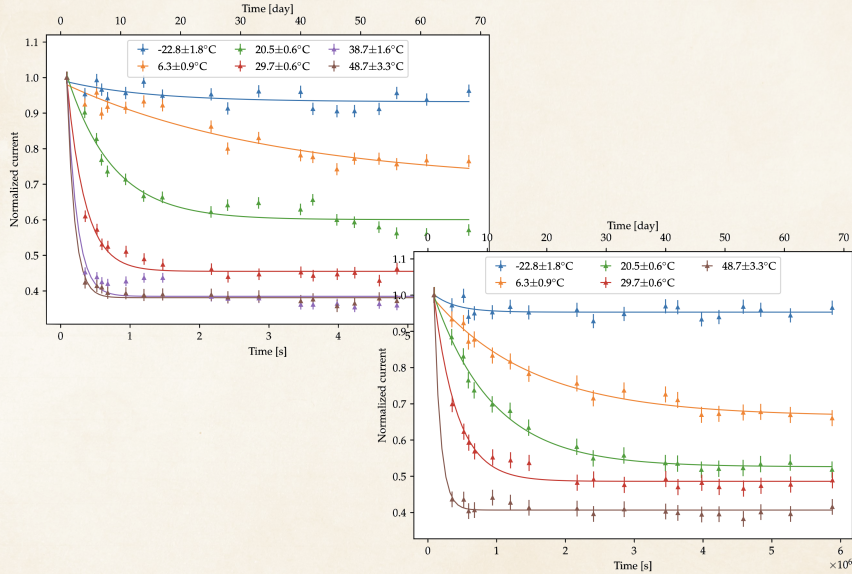
SiPM Dose Map POLAR-2



Time evolution of dark current at $\Delta V=3$ V 25 and 50 μm microcells

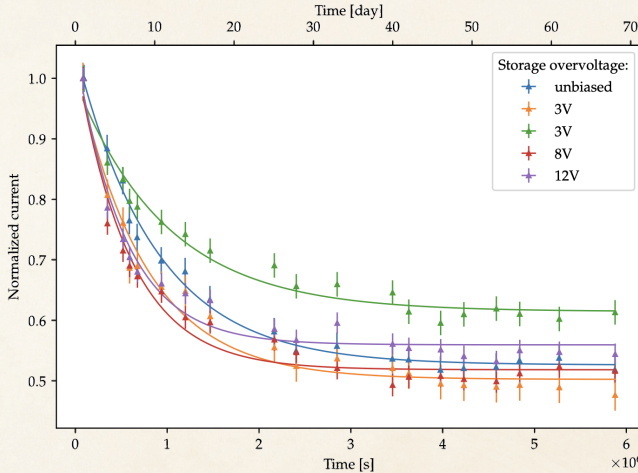


Time evolution of dark current at $\Delta V=3$ V 25 and 50 μm microcells

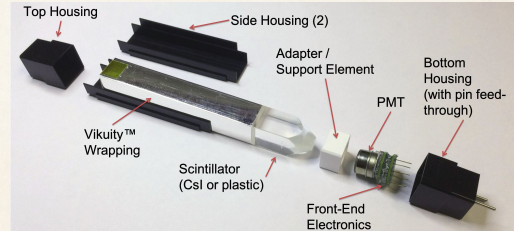
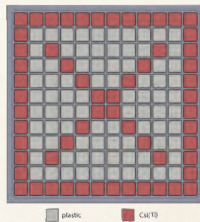
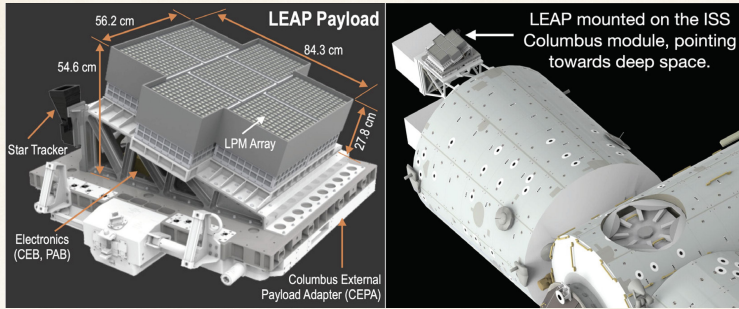


Annealing with biased sensors

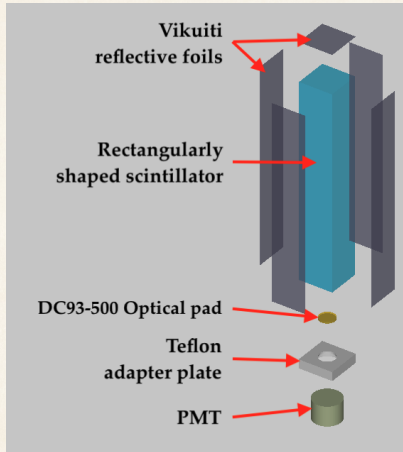
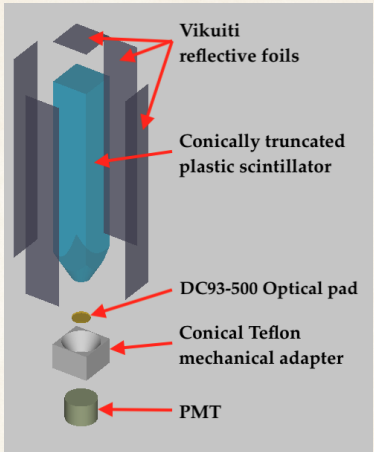
Behavior is the same as for unbiased SiPMs (S13360-6050PE):



LEAP design

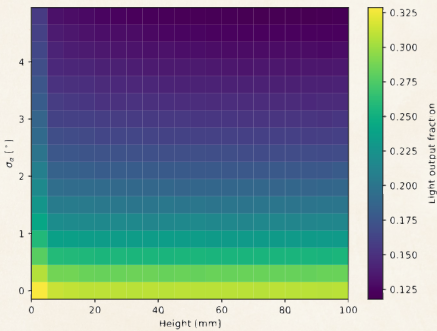
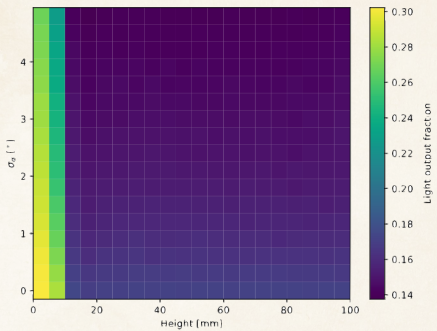


LEAP PDE Optical Simulation



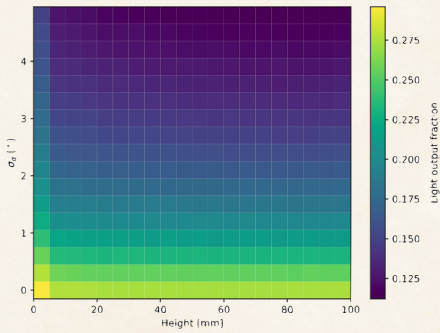
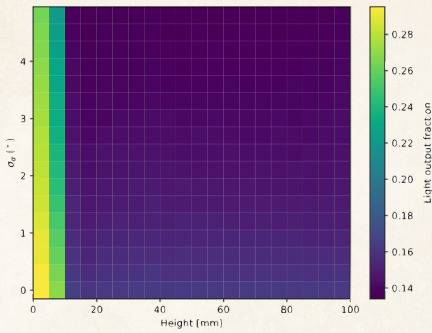
Simulated LEAP Light Output

EJ-200

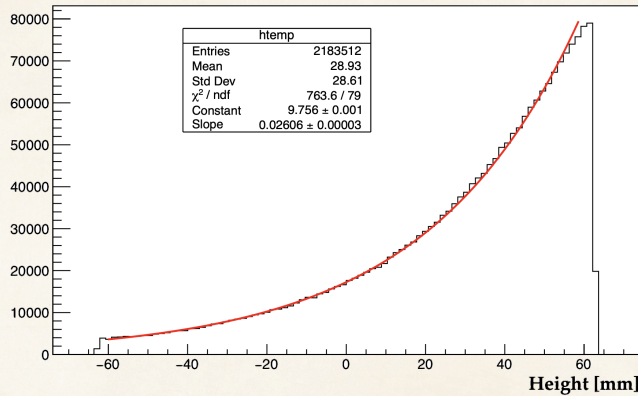


Simulated LEAP Light Output

EJ-248M



Simulated LEAP Light Output Comparison



	EJ-200	EJ-248M
Conically tapered bar	$14.21 \pm 0.04\%$	$14.40 \pm 0.04\%$
Square bar	$13.85 \pm 0.04\%$	$17.71 \pm 0.04\%$